Adsorbed layer structure of cationic surfactants on quartz

Jamie C. Schulz and Gregory G. Warr*
School of Chemistry, The University of Sydney, Sydney, NSW 2006, Australia

Paul D. Butler
NIST Center for Neutron Research, National Institute of Standards and Technology, 100 Bureau Drive, Gaithersburg, Maryland 20899-8562

W. A. Hamilton
Solid State Division, Oak Ridge National Laboratory, Oak Ridge, Tennessee 37831-6393
(Received 3 August 2000; published 29 March 2001)

Recent atomic force microscopy (AFM) surface images of surfactant adsorbed at solid and solution interfaces have shown apparent micellar aggregates familiar from bulk self-assembly. This contradicts the classical picture of laterally unstructured bilayers within which neutron reflectometry (NR) measurements have previously been analyzed. Applying both techniques to surfactant adsorption on quartz, we show that film thickness and coverage parameters derived from NR results are generally consistent with those from AFM and bulk self-assembly. NR by itself allows us to distinguish between actual bilayer and probable aggregate adsorption, which will be of particular importance when a solution's rheology makes AFM imaging impractical.

DOI: 10.1103/PhysRevE.63.041604 PACS number(s): 68.43.−h, 82.65.+r, 61.12.Ha, 68.55.Jk

Knowledge of adsorbed layer structure is important in many classical colloidal applications including mineral flotation [1] and detergency [2] where adsorbed layer morphology may impact directly on the success of a particular formulation. From a different perspective, recent studies of mesoporous silicate formation, in bulk [3] and at interfaces [4], have also raised the question of how adsorbed layer and bulk self-assembly structures are related, and in particular how far the curvature of a bulk aggregate can be compromised as precipitation of an adjacent solid proceeds.

Traditionally, adsorbed surfactant on a mineral oxide has been viewed as a laterally structureless bilayer. For a cationic surfactant on a negatively charged surface such as quartz, electrostatic interactions between a surfactant head group and a solid surface drive an initial adsorption step which leaves surfactant alkyl tails exposed to water. A second layer is then presumed to form, driven by hydrophobic attractions and giving rise to surfactant molecules with head groups exposed to water and hydrophobic tails sequestered away from water as in a free bilayer [see Fig. 1(C)] [5]. This model of an adsorbed layer is at odds with the known bulk self-assembly behavior of amphiphilic molecules. Here molecular packing considerations are dominant, leading to the formation of spherical or cylindrical micelles or bilayer structures even in dilute solution [6]. Bulk solution self-assembly is now fairly well understood, but can this be translated to an understanding of adsorbed layer structure?

Recent atomic force microscopy (AFM) studies have revealed a plethora of largely unanticipated morphologies of adsorbed surfactant layers at solid and solution interfaces, particularly graphite and mica [7]. Cylinders or hemicylinders are most commonly reported [8], with spheres and laterally unstructured (bilayer) films also observed, suggesting that adsorbed layer structure may have something in common with bulk self-assembly. On the other hand, neutron reflectometry (NR) studies [9], despite some anomalies [10], are generally reported to be consistent with the conventional bilayer view of adsorbed surfactants [5,11]. To some extent this contradiction has persisted, because the atomically flat graphite and mica substrates to which AFM observations have largely been restricted are not easily amenable to other methods of experimental investigation. It might also be argued that the unusual nature of these substrates would explain the different interpretations of adsorbed layer structure. However, it is not essential for AFM that a substrate be atomically smooth. The necessary requirement is only that the surface is not rough on the same length scale as any lateral structure in the adsorbed layer. Parallel AFM and NR studies of surfactant adsorption onto crystalline quartz are reported below, from which we develop a consistent picture of the adsorbed film formed by cationic surfactants under a variety of solution conditions which are known to lead to different aggregate shapes in bulk.

AFM imaging of surface aggregates was carried out in the noncontact mode, as described previously [12]. Surfactant solutions were introduced into the AFM fluid cell, and imaging was carried out in situ with the AFM tip deflected due to electrostatic interactions with the adsorbed layer on the substrate. The imaging force was maintained below that required to break through the adsorbed film, as determined from the force-distance curve between the AFM tip and quartz substrate [13]. Neutron reflectometry experiments were performed at Oak Ridge National Laboratory using the MIRROR beam line [14]. Surfactant solutions were prepared in D_2O or a contrast-matched D_2O/H_2O mixture (i.e., one whose average neutron scattering length density was the same as that of quartz, $4.17\times10^{-4}\,\mathrm{nm}^{-2}$). Specularly reflected intensities for a neutron beam passing through a

*Author to whom correspondence should be addressed; electronic address: g.warr@chem.usyd.edu.au

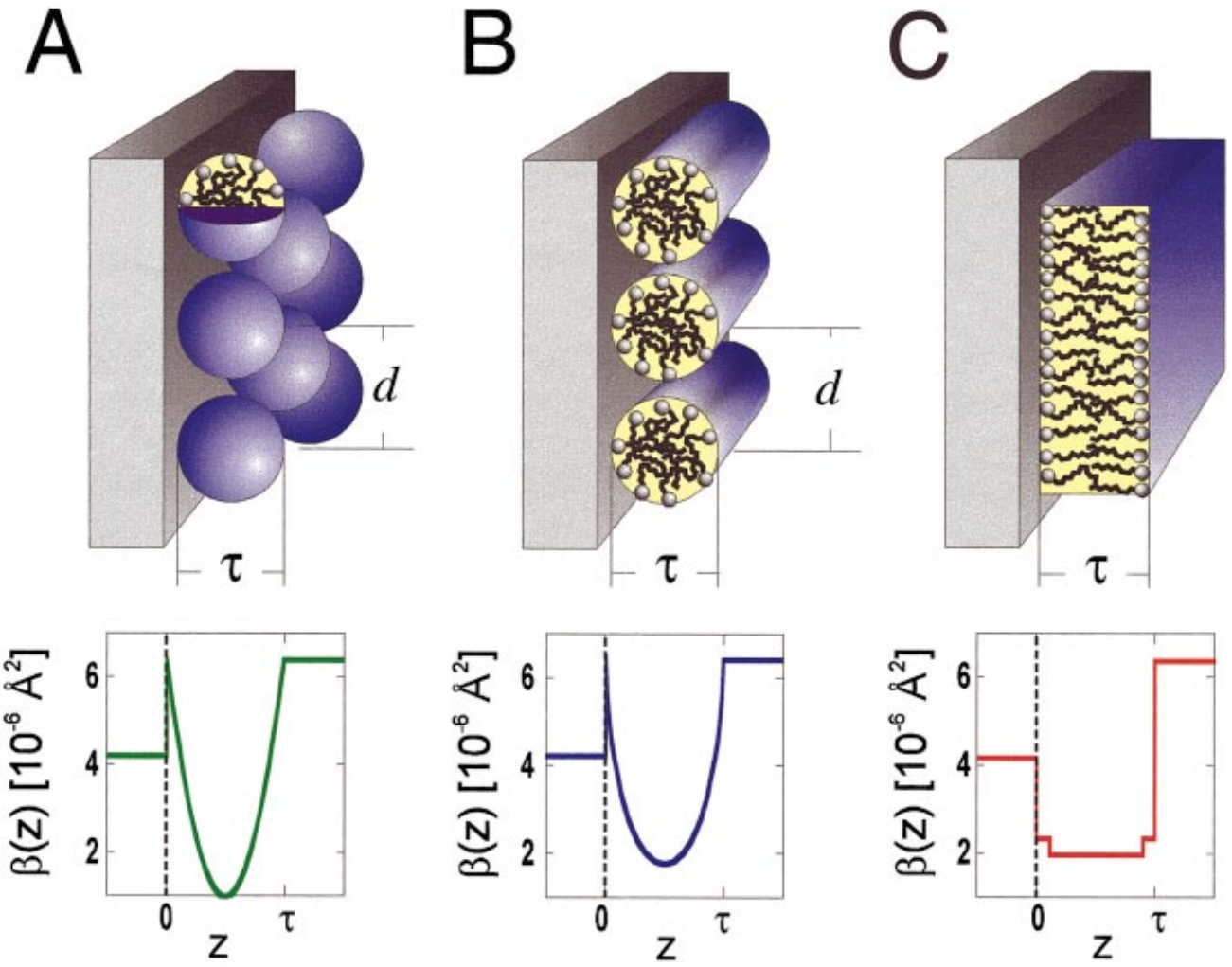

FIG. 1. (Color) Schematic diagram of adsorbed layer structures consisting of (A) spherical micelles, (B) cylindrical micelles, and (C) a bilayer, including the film thickness τ and interaggregate spacing d. Also shown are examples of neutron scattering length density profiles normal to the interface, $\beta(z)$, corresponding to each structure at the quartz/D_2O interface at a fractional surface coverage of 0.55. The head-group and alkyl tails of the surfactants have different scattering length densities, but because of the arrangement of the molecules this is only apparent in the bilayer $\beta(z)$.

single-crystal quartz block and reflected from the quartz-solution interface were recorded as a function of angle of incidence. The off-specular background, including any signal due to scattering from the bulk solution [15], was subtracted to give the reflection coefficient of the surfactant-coated interface. All solutions used were above their critical micelle or aggregation concentration, a condition which leads to a saturated adsorbed film at the solid-solution interface.

The cationic surfactant tetradecyltrimethylammonium bromide (TTAB) forms nearly spherical micellar aggregates consisting of approximately 80 molecules in bulk solution. Small angle neutron-scattering measurements [16] give mi-

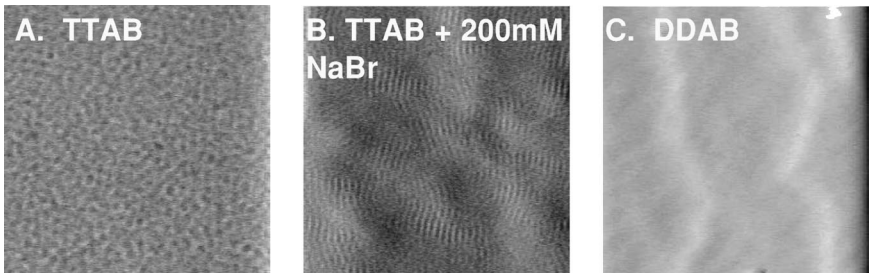

FIG. 2. 200×200-nm^2 AFM tip deflection images of (A) spherical TTAB aggregates adsorbed onto quartz from water solution, (B) cylindrical TTAB aggregates adsorbed onto quartz from an aqueous 200mM NaBr solution, and (C) planar DDAB bilayer adsorbed onto quartz from water solution. Long-wavelength undulations visible in (B) and (C) arise from roughness in the underlying quartz.

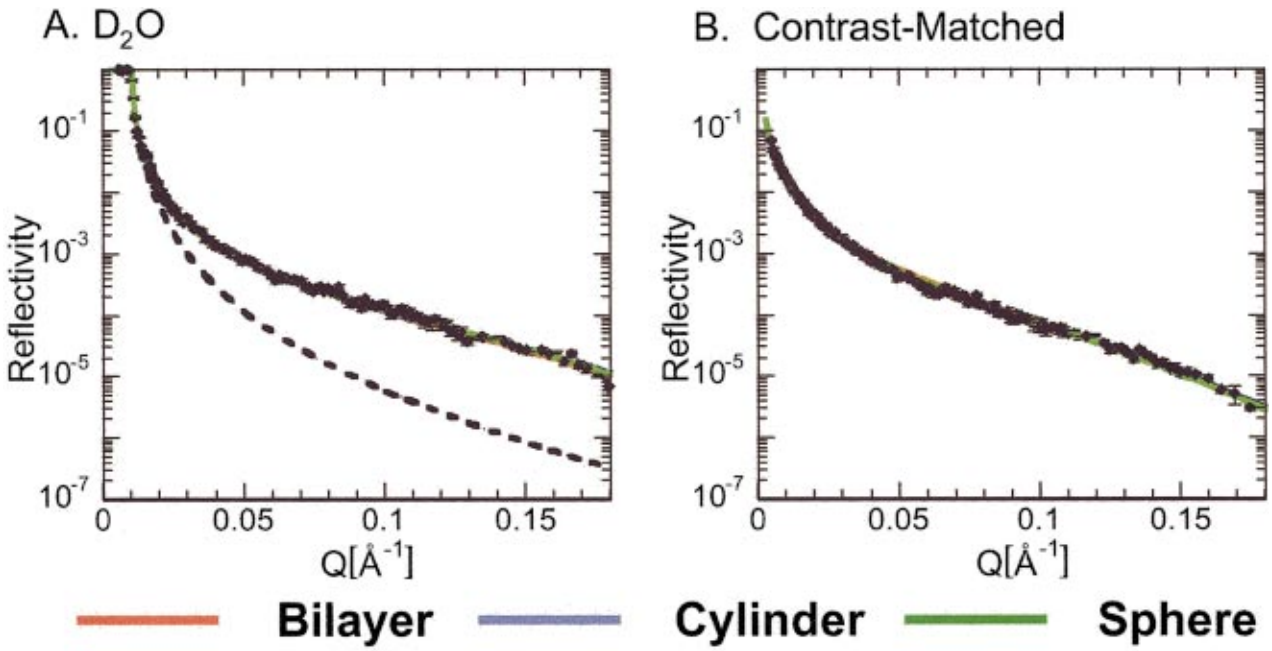

FIG. 3. (Color) NR results for DDAB adsorbed onto quartz from (A) D_2O and (B) a D_2O/H_2O mixture contrast matched to quartz. Solid lines show the (virtually indistinguishable) best fits of sphere, cylinder, and bilayer models for the adsorbed layer corresponding to the derived parameters listed in Table I. The dashed line in (A) is the reflectivity from clean quartz.

cellar diameters of 5.4 ± 0.3 nm. AFM of the adsorbed layer of TTAB [Fig. 2(A)] on quartz shows an array of circular dots. The average nearest-neighbor distance obtained from this particular image was 6.9 ± 0.5 nm. As expected, this is somewhat greater than the bulk micelle diameter; the distance includes the diameter of the spherical micelle plus separation due to intermicellar electrostatic repulsion. Addition of NaBr to TTAB solutions is known to induce a sphere-to-cylinder transition in the micelles at a concentration of 120 mM [17]. This too is observed in the adsorbed layer, with the shape transition visible at 90-mM NaBr [18]. Figure 2(B) shows the adsorbed layer of TTAB on quartz in 200-mM NaBr to consist of parallel meandering stripes consistent with full cylindrical micelles. The spacing between these micelles is 4.9 ± 0.5 nm. In order to generate a true bilayer adsorbed film we chose the double-chained surfactant didodecyldimethylammonium bromide (DDAB), which forms bilayer structures directly in bulk solution [19], and indeed the AFM image of its adsorbed layer shows a laterally homogenous film with no periodic structures [Fig. 2(C)]. Coverage of the surface appears to be complete, with no patches or holes evident.

In all cases we note that the AFM results indicate a similarity between adsorbed layer structures and those familiar in bulk self-assembly. NR experiments on the same surfactant systems but in D_2O and a D_2O/H_2O mixture contrast matched to quartz also reveal the presence of adsorbed surfactant. Whereas AFM yields a detailed picture of lateral structure, it provides little in the way of quantitative information, and little about the adsorbed layer structure normal to the interface. NR is sensitive to the details of the scattering length density profile normal to the interface, and can be used to unambiguously obtain the amount of adsorbed surfactant, Γ. NR results were fitted to three models for the adsorbed layer: spheres, cylinders, and a laterally homogeneous layer (a bilayer), as shown schematically in Fig. 1. Each model has a unique scattering length density profile $\beta(z)$, which contains two parameters: an overall film thickness τ, and a volume fraction of surfactant in the adsorbed layer [20]. In the case of regular adsorbed structures such as cylinders or spheres, these parameters can be related to a nearest-neighbor distance, d (Fig. 1). Figure 3 shows fits of all three models to the reflectivity curves using as an example the bilayer-forming DDAB. Obviously it is not possible to distinguish the adsorbed layer structure solely on the basis of goodness of fit; adsorbed cylinders, spheres, and bilayers all seem plausible. A similar goodness of fit was observed for the TTAB reflectivity data both with and without electrolytes. The best-fit parameters for each of these models are summarized in Table I.

The models of the adsorbed film structure are discriminated using bulk solution contrast variation. The fitted parameters and the derived surface excesses must agree for both solution contrasts. Furthermore it is expected that the thickness of the adsorbed film will be similar to the bulk solution aggregate dimensions, and that electrostatic repulsion between aggregates in films composed of spheres or cylinders will result in a separation between aggregates. Intuitively it is also expected that the fractional surface coverage of a genuine bilayer forming surfactant will be complete (i.e., unity), and hence consistent with the AFM image shown in Fig. 2(C). The interfacial model which best fulfills these criteria for each system are shaded in Table I.

As Table I shows, the surface coverage or amount adsorbed determined by NR is independent of the model for the adsorbed layer when quartz and solution are contrast

TABLE I. Fits to adsorbed layer structure for cationic surfactant systems on quartz from neutron reflectometry. Consistent fits to NR and AFM images for each system are set in bold, showing agreement between adsorbed amounts in the D_2O and quartz contrast-matched D_2O/H_2O measurements. Also listed are the film thicknesses τ and nearest-neighbor spacings d, from NR fitting and AFM images, showing agreement between the two techniques for the best fit NR case.

		NR in D_2O			NR in contrast-matched D_2OH_2O			AFM
		Γ (μmol m^2)	d (nm)	τ (nm)	Γ (μmol m^2)	d (nm)	τ (nm)	d (nm)
TTAB	**Spheres**	**6.6±0.6**	**5.3±0.3**	**4.6±0.4**	**6.5±0.4**	**5.2±0.3**	**4.6±0.3**	**6.9±0.5**
	Cylinders	6.1±0.6	5.1±0.5	3.6±0.4	**6.4±0.3**	6.0±0.3	4.0±0.2	
	Bilayer	5.4±0.5		2.7±0.3	**6.4±0.3**		3.3±0.1	
TTAB+200 mM NaBr	Spheres	7.3±0.3	5.2±0.2	4.7±0.1	**6.9±0.3**	4.7±0.2	4.4±0.2	
	Cylinders	**7.0±0.4**	**5.5±0.3**	**4.0±0.2**	**6.9±0.3**	**5.2±0.2**	**3.9±0.2**	**4.9±0.5**
	Bilayer	6.3±0.4		3.0±0.2	**6.8±0.3**		3.2±0.1	
DDAB	Spheres	4.7±0.3	3.0±0.2	3.2±0.2	**4.9±0.2**	3.5±0.2	3.6±0.2	
	Cylinders	4.5±0.3	2.5±0.2	2.6±0.2	**4.8±0.2**	3.3±0.1	3.1±0.1	
	Bilayer	**4.2±0.2**		**2.1±0.2**	**4.8±0.2**		**2.6±0.1**	‘

matched [21]. However, different adsorbed layer structures in D_2O yield different fitted adsorbed amounts in two of the three cases shown. For TTAB with and without added electrolytes, the bilayer structure can be eliminated. The best-fit NR adsorbed amounts also agree with results from adsorption isotherms for TTAB on silica at natural pH [22], and the increase in adsorbed amount with addition of salt is consistent with expectations. Added salt electrostatically screens interactions between adsorbed micelles, allowing them to pack more closely together and, in the case shown, induce a sphere-to-cylinder transition. Adsorbed amounts can also be converted to a fractional surface coverage using the molar volumes of adsorbed surfactants. NR shows that bilayer-forming DDAB has a fractional coverage of 0.98 ± 0.02, which is consistent with the complete surface coverage observed by AFM. TTAB, both with and without added electrolytes, has much lower fractional surface coverages. TTAB alone has a surface coverage of 0.46 ± 0.02 (sphere fit), and with 200-mM electrolyte 0.50 ± 0.03 (sphere fit) or 0.57 ± 0.02 (cylinder fit). This less than unity surface coverage has previously been rationalized as a ‘‘patchy bilayer’’ [9] or a partial surface coverage. Such fractional surface coverages are a natural consequence of the existence of adsorbed micelles which can pack to a geometrical maximum fraction of 0.60 for spheres or 0.79 for cylinders.

Table I lists nearest-neighbor spacings for various adsorbed structures derived from NR and AFM. Values for the various TTAB measurements agree reasonably well, considering that d is derived indirectly from NR, whereas AFM reveals the lateral aggregate arrangement on the surface directly. Also note the agreement between film thickness and bulk micelle diameter for TTAB with no added salt [16]. The adsorbed (Table I) and free bilayer thicknesses for DDAB (2.4 ± 0.1 nm from small angle x-ray scattering [23]) are likewise in good agreement with each other. Also telling is that the micellar fits for the DDAB adsorbed layer give d values very close to those for τ, requiring that the charged surfaces of the supposed adsorbed micelles are in contact with those of their neighbors. This unrealistically tight packing is another indicator of a true bilayer structure for this adsorbed film. To summarize the information available from the NR results: for TTAB and TTAB+NaBr the paired measurements give surface coverages, layer thickness, and packing separations calculated assuming micellar aggregate adsorption that are consistent (e.g., $d>\tau$), while if we assume a bilayer the surface coverage results for D_2O disagree with the definite value given by the contrast-matched samples; for DDAB, while the surface coverage values are in general agreement for all models, the full surface coverage calculated from the molar volume assuming a bilayer (0.98 ± 0.02) and the overly close packing if we assume micellar structures ($d\simeq\tau$) strongly suggest the former morphology. Throughout the film parameters thus obtained agree well with the dimensions of bulk surfactant structures. While discriminating between spherical and cylindrical adsorbed micelles is not possible by NR alone [24]; clearly it is possible to distinguish between adsorbed bilayers and adsorbed micellar aggregates solely from NR data at different solution contrasts on the basis of physically reasonable surface coverages and putative intermicellar spacings. We note that this degree of complementarity between NR and AFM observations can be expected to assume greater importance in determining adsorbed surfactant morphologies when the solution’s rheology makes AFM imaging impractical (for example, viscoelastic solutions [10]).

In conclusion, a self-consistent interpretation of our AFM and NR measurements yields a picture of fully developed adsorbed layers of micelle- and bilayer-forming surfactants on quartz. Both techniques reveal adsorbed films of micelle-forming surfactants which exist as arrays of micelles with individual structures corresponding closely to those present in bulk solution. Only for the surfactant that self-assembled

into bilayers in the bulk did we observe a true adsorbed bilayer. Overall, it appears that surface adsorption alters intrinsic curvature of surfactant aggregates less than might have been expected and that the head group packing parameters invoked to explain bulk self-assembly morphologies [6] still dominate in the adsorbed layer. We expect that a similar situation will apply to other mineral oxides.

We acknowledge the support of the Australian Research Council (G.G.W.) and the Australian Nuclear Science and Technology Organization (G.G.W. and J.C.S.). J.C.S. acknowledges financial support from the University of Sydney. P.D.B. acknowledges support from U.S. National Science Foundation Grant No. DMR-9423101. During this work Oak Ridge National Laboratory has been managed for the U.S. Department of Energy by Lockheed Martin Energy Research Corporation under Contract No. DE-AC05-96OR22464 and by UT-Batelle LLC under Contract No. DE-AC05-00OR22725.

[1] A. M. Gaudin and D. W. Fuerstenau, Trans. AIME **202**, 958 (1955).

[2] *Detergency: Theory and Technology*, edited by W. G. Cutler and E. Kissa, Surfactant Science Series Vol. 20 (Dekker, New York, 1986).

[3] C. T. Kresge *et al.*, Nature (London) **359**, 710 (1992).

[4] A. S. Brown *et al.*, Langmuir **14**, 5532 (1998).

[5] B. H. Bijsterbosch, J. Colloid Interface Sci. **47**, 186 (1974).

[6] J. N. Israelachvili, D. J. Mitchell, and B. W. Ninham, J. Chem. Soc., Faraday Trans. 2 **72**, 1525 (1976).

[7] S. Manne and H. Gaub, Science **270**, 1480 (1995).

[8] W. A. Ducker and E. J. Wanless, Langmuir **15**, 160 (1999); R. Lamont and W. A. Ducker, J. Colloid Interface Sci. **191**, 303 (1997); N. B. Holland, M. Ruegsegger, and R. E. Marchant, Langmuir **14**, 2790 (1988); W. A. Ducker and E. J. Wanless, *ibid.* **12**, 5915 (1996); S. Manne *et al.*, *ibid.* **13**, 6382 (1997).

[9] D. C. McDermott *et al.*, Langmuir **9**, 2404 (1993); D. C. McDermott *et al.*, J. Colloid Interface Sci. **162**, 304 (1994); J. Penfold *et al.*, Langmuir **13**, 6638 (1997).

[10] P. D. Butler *et al.*, Faraday Discuss. **104**, 65 (1996); **104**, 88 (1996).

[11] L. G. T. Eriksson *et al.*, J. Colloid Interface Sci. **181**, 476 (1996); H. P. Hankins and J. H. Ohaver, Ind. Eng. Chem. Res. **35**, 2844 (1996); T. P. Goloub and L. K. Koopal, Langmuir **13**, 673 (1997); M. Szekeres, I. Dekany, and A. de Keizer, Colloids Surf., A **141**, 327 (1998).

[12] S. Manne *et al.*, Langmuir **10**, 4409 (1994).

[13] H. N. Patrick *et al.*, Langmuir **15**, 1685 (1999).

[14] W. A. Hamilton, J. B. Hayter, and G. S. Smith, J. Neutron Res. **2**, 1 (1994); M. Yethiraj and J. A. Fernandez-Baca, in *Neutron Scattering in Materials Science II*, edited by D. A. Neuman, T. P. Russell, and B. J. Wuensch, MRS Symposia Proceedings No. 376 (Materials Research Society, Pittsburgh, 1995).

[15] The MIRROR reflectometer has a one-dimensional detector allowing simultaneous measurement of the specular reflection signal and off-specular scattering in the reflection plane. The background in the specular reflection region due to small angle scattering of the transmitted beam in the bulk [see, for instance, W. A. Hamilton *et al.*, Physica B **221**, 309 (1996)] can therefore be determined from interpolation of a fit to the scattering in the off-specular regions on either side of the reflected beam.

[16] S. S. Berr, J. Phys. Chem. **91**, 4760 (1987).

[17] T. Imae and S. Ikeda, J. Phys. Chem. **90**, 5216 (1986).

[18] To our knowledge this is the first reported observation of a salt-induced sphere-to-cylinder transition in adsorbed surfactant aggregates.

[19] G. G. Warr, R. Sen, D. F. Evans, and J. E. Trend, J. Phys. Chem. **92**, 774 (1988).

[20] J. C. Schulz *et al.*, J. Phys. Chem. B **103**, 11 057 (1999).

[21] The consistency of the values obtained for the adsorbed amount per unit area Γ between the various models under contrast matched conditions may be understood by consideration of a Guinier-like (low wave-vector Q, low reflectivity R) approximation to the reflectivity in this situation due to Crowley (T. L. Crowley, Ph.D thesis, Oxford University, 1984). In terms of the quantities used in this paper we may write $R \approx 16\pi^2(\Gamma\Delta\beta\, V_m^2/Q^2)\exp[-\sigma^2Q^2]$. We see that Γ determines the magnitude of the reflectivity at low Q, since, multiplied by the ratio of the scattering length density contrast between the adsorbate and the surrounding media ($\Delta\beta$) and its molar volume (V_m) it gives the total surface scattering power appearing in the leading term. This is independent of morphology, which enters into the exponential term as σ, the mean square deviation of the adsorbate contrast profile, and simply modifies the falloff from the low Q limit.

[22] P. Wägnerud and G. Olofsson, J. Colloid Interface Sci. **153**, 392 (1992).

[23] M. Dubois and Th. N. Zemb, Langmuir **7**, 1352 (1991).

[24] This is to be expected, given the similarity in the scattering length density profiles of adsorbed spherical and cylindrical aggregates (cf. Fig. 1).